EFFECTS OF MOISTURE MIGRATION ON SHRINKAGE, PORE PRESSURE AND OTHER CONCRETE PROPERTIES

D. A. CHAPMAN, G. L. ENGLAND

Department of Civil Engineering, King's College, University of London, Strand, London WC2R 2LS, United Kingdom

SUMMARY

This work investigates the uniaxial migration of moisture in long, upright, limestone concrete cylinders, sealed at the base and sides, and open at the top. The design represents a section through a concrete pressure vessel wall.

The cylinders are subjected to a sustained temperature difference between their ends, with maximum temperatures between 105 °C and 200 °C. Readings of pore pressure, water content and temperature are taken at various positions along the axis of the cylinders. In one cylinder, transverse and longitudinal shrinkage readings are also recorded.

The results for the cylinders show that moisture migration is away from the hot face of the specimens, causing reduction in both pore pressure and water content values in this region. The moisture migration creates a drying front which moves slowly up the specimens. The rate at which this drying front moves is influenced by the base temperature, the magnitude of temperature and pressure gradients and the coefficient of permeability of the concrete. Samples taken from the hot side of the drying front show a considerable increase in the coefficient of permeability, and Scanning Electron Microscope photographs of the microstructure show both a break-up and reduction in size of the hydration products.

Preceeding the hot drying front are waves of moisture resulting in "wet" regions in the centre of the specimens, where the total water content becomes greater than at the time of mixing. Scanning Electron Microscope photographs of samples from these "wet" regions indicate that the elevated temperatures and excess moisture enhance the concretes' hydration. Values of the coefficient of permeability are in the order of 100 times less than those for the hot side of the drying front.

Evaporation drying takes place from the unsealed end of the specimen. A drying front moves into the concrete and considerable weight loss is recorded as moisture escapes to the atmosphere. The rate of movement of the drying front is slower than that of the hot front and is proportional to the temperature difference between the top of the specimen and the surrounding atmosphere.

In the shrinkage specimen, values of transverse and longitudinal shrinkage reflect the water content results. The specimen indicates that shrinkage occurs in a concrete pressure vessel, in the regions where moisture is lost. The restraint of the mass of concrete surrounding these regions sets up a three dimensional state of internal tensile stress. The areas into which the moisture migrates tend to swell, creating an internal stress situation, which is this time compressive. These results indicate that if shrinkage strain values for concrete pressure vessels are calculated by subtracting the initial thermal movement from the total predicted movement, a higher value is obtained than occurs in practice.

The experiments reported indicate that when the hot inner face temperature of a concrete pressure vessel is increased above 100 °C, the drying rate inside the wall increases considerably. However, it is unlikely pressure vessels of the size currently in use will ever completely dry out.

1. Introduction

The adoption of the Prestressed Concrete Pressure Vessel design for nuclear reactors has permitted an integral design, with the entire gas circuit, including boilers, contained within a single pressure envelope. Better safety and resultant economy have been achieved, and the provision of a separate biological shield obviated. The thickness of concrete in the pressure vessel is usually in the range 10 ft. - 20 ft., and is sufficient to reduce any harmful radiation to a safe level. Maximum radiation protection and safety is obtained with the highest possible moisture content spread evenly over the cross-section of the wall.

Since the Energy crisis of 1973, attention has been refocussed on the development of nuclear power, with special reference to the efficiency of the present systems in use, and where cost economies can be applied. System efficiency can be increased by raising the working temperatures and pressures inside the reactor. Cost economies can be effected by a reduction in the volume of the costly cooling and insulation systems. Both these actions would increase the maximum temperature of the concrete, which in present systems is generally in the 60°C to 80°C region. These actions would also increase the movement of moisture in and from the concrete pressure vessel wall.

During the past decade, a series of experimental studies, [1,2,3,4,5] have been carried out at King's College, London into moisture migration in and from concrete specimens under a thermal gradient and its effect upon various physical and engineering properties of concrete. Ross, Illston and England [1], found that on a simulated thick-wall section, sealed at the hot face and subjected to a thermal gradient of 12°C/ft., drying had only taken place in the foot of concrete adjacent to each face after one year of heating. Sharp [2] investigated this in more detail with sealed cylindrical specimens in lengths ranging from 2 ft. to 10 ft. open at one end to atmosphere, and heated for 2 years at their bases to temperatures of 80°C, 105°C and 135°C. He observed that penetration of the drying front at the hot end was temperature related. Depending on the length of the moisture path, water content values in excess of the mixing water values were observed in the intermediate regions of the specimen. Evaporation drying took place at the ends open to atmosphere. A typical phase diagram for water in such specimens was produced by England and Ross [3], and can be seen in figure 1.

Similar migration studies to those of Sharp have been reported by Hornby [6] and Mcdonald [7], neither of whom observed these areas of increased water content. However, Hundt and Schimmelwitz [8], in a sealed moisture migration specimen with a hot face temperature of 80°C, observed an area in the intermediate region of the specimen with a small increase in moisture content over the moisture content before heating.

Parkinson [4] investigated water movement and any accompanying shrinkage in sealed concrete subjected to a thermal gradient. Measurements of moisture content showed an accumulation of water in the cool regions and this was accompanied by "swelling" of the concrete. This "swelling" phenomena was also reported by England and Ross [3] in a series of laminated specimens subjected to a thermal gradient and unidirectional moisture flow.

England and Sharp [5] reported measured pore pressures at various points along the axes of sealed cylindrical specimens under the action of sustained thermal gradients. The pore pressures were observed to dissipate slowly in the hot regions as water migrated towards the

cooler parts of the specimen, and were indicators of the changing water content in the specimens. They concluded that at temperatures in excess of 100°C, the pore pressures became significant and major factors affecting the movement of moisture.

The experimental work reported in this paper must be viewed as an extention of the moisture migration studies conducted at King's College. Two series of experiments are reported. The objectives of these were:

(i) To extend the moisture migration tests previously performed at King's College, with larger scale specimens and at higher maximum concrete temperatures. This was to simulate increasing the system efficiency and introducing cost economies into a nuclear reactor design.

(ii) To combine observations of pore pressure, moisture content and shrinkage from a single cylindrical concrete specimen under a thermal gradient.

Limestone concrete was used in all the tests. This type of concrete is favoured for use at high temperatures in concrete pressure vessels [9].

2. Experimental Programme

The cylinders used in the first series of tests were of two lengths, 5 ft. and 10 ft. and of 6" diameter. The sealing jackets used were of mild steel tubing. The specimens were cast vertically, using a mix of 1½:4:6 (Ordinary Portland Cement : sand : aggregate). The water : cement ratio was 0.6 and the fine and coarse aggregates were of limestone. The specimens were instrumented throughout their length with thermocouples, moisture meters and pressure tappings as described elsewhere [10], and were subjected to sustained heating at their lower ends. The upper cool ends of the test specimens were unsealed and consequently moisture was allowed to escape freely to the atmosphere. Table 1 lists the testing conditions of each specimen in the series.

Readings of Pore Pressure, Temperature and Evaporable water content were recorded, and loss of moisture from the specimens monitored by direct weighing throughout the periods of heating. After heating had ceased, samples of concrete were removed immediately from various positions along the axes of all the specimens. These samples were used to determine the evaporable and non-evaporable water distributions by gravimetric measurements [11]. Additionally, samples were removed from all the 5 ft. specimens for viewing under a Scanning Electron Microscope, while samples from B2 and D4 were also used for permeability measurements.

The specimen used to monitor shrinkage values in addition to the other parameters measured in the first series was a cylinder of 10" diameter and 5 ft. long. This was cast using the same mix, in a series of 3" discs. Similar instrumentation to that used in the first experimental series was cast into each disc, with the addition of brass surface studs to measure the horizontal and vertical movements of the concrete. A sealing jacket of silicone rubber was used, bonded to the outer concrete surface to prevent moisture loss, but still permitting the concrete to move, and shrinkage to be recorded. The whole specimen was then encased in a steel jacket. Any gap between the rubber and steel was filled with grout. The unheated top of the specimen was left open to atmosphere, and the lower sealed end was heated electrically. The thermal gradient produced along the axis of the specimen is shown in Figure 2. Readings of Temperature, Pore Pressure, Evaporable water content, Transverse

and Longitudinal shrinkage in each disc were recorded throughout the heating period, which lasted 495 days. Samples of the concrete were removed after heating had ceased and used to determine the evaporable and non-evaporable water distribution, as in previous tests.

A subsidiary control experiment to determine the variation of the coefficient of linear expansion with evaporable water content was run simultaneously with the shrinkage experiment. The purpose of this experiment was to enable the true shrinkage values to be determined more accurately as the evaporable water content in each disc changed. The experiment consisted of a laminated specimen of eleven slices. Into each slice, a moisture meter and brass surface studs were cast. The edges of the slices were sealed so that moisture migrated from one slice to the next due to the imposed thermal gradient. The strain changes caused by the migrating moisture allowed the variation of linear coefficient of thermal expansion to be evaluated.

3. Experimental Results

Only a selection of results of the comprehensive study [11] is presented here but the reader is referred to a fuller set of results from these experiments, to be published shortly [12, 13, 14]. Figure 3 gives the phase diagram for water in migration specimen B2 at the end of the time of heating. This diagram is typical for all the migration specimens and the shrinkage specimen. Figure 4 illustrates the total water content distribution for all the 5 ft. migration series specimen at the end of heating obtained by gravimetric measurements. The 10 ft. migration series produced a similar set of curves. Figure 5 is a plot of the loss in weight from each of the 5 ft. migration series specimens against time of heating. Figure 6 gives a typical set of pore pressure distributions at various ages of heating; these are for specimen B2. Table 2 lists the values of measured D'Arcy coefficients of permeability in various samples of concrete from specimens B2 and D4 of the 5 ft. migration series. The temperature of the sample in the specimen and the weights of Evaporable, $\left(\frac{W_E}{W_T}\right)$, Non Evaporable, $\left(\frac{W_N}{W_T}\right)$, and total water, all expressed per unit weight of mix water, are also listed.

Four scanning electron micrographs are presented to illustrate briefly some of the trends observed in the microstructure of the concrete in the migration series specimens. Table 3 lists the temperature of the sample of concrete viewed, as it was in the migration specimen, the base temperature of migration specimen, and the Evaporable $\left(\frac{W_E}{W_T}\right)$, Non-Evaporable $\left(\frac{W_N}{W_T}\right)$ and total water content, per unit weight of mix water.

A full report giving the results observed in the scanning electron micrographs of the migration specimens is planned for publication by the authors in a separate paper.

Figure 7 shows the recorded variation of the linear coefficient of thermal expansion with evaporable water content for the limestone concrete. Figure 8 shows transverse shrinkage strains in Disc 2 of the shrinkage specimen, and Figure 9 gives the distributions of water content, pore pressure, transverse and longitudinal shrinkage after 100 days and 495 days of heating.

4. Discussion of Results

The phase diagrams for the water in all the specimens were obtained by removing samples

of concrete at the end of heating and determining the Evaporable and Non-Evaporable water distributions of gravimetric measurements. Figure 3 is for specimen B2, a 5 ft. migration specimen with a hot end temperature of 125°C, heated for 588 days. The cross-hatching represents the area where the total water content was greater than at the time of mixing. The length of these 'wet' regions in all the migration series specimens decreased as the hot end temperature increased. In all the specimens, the maximum value of the non-evaporable water content occurred in these 'wet' regions. In most of the specimens, the non evaporable water content was essentially constant over the central portion and deviated only in the regions 6 in. from either end. Here, the values were lower. This was due clearly to a combination of effects. Water was forced to migrate from the hottest regions and was free to escape to the atmosphere from the coolest parts, thus leaving the two extremities of the specimens in a relatively dry state. The central portion of the concrete, however, was subjected to sustained moist conditions and in consequence hydration would be enhanced in these areas relative to the two ends.

Figure 4 gives the total water content distributions for the 5 ft. migration series specimens. This figure indicates that the movement of the 'hot' drying front is influenced by the magnitude of the base temperature. In both the 5 ft. and 10 ft. specimens, the distance moved by the 'hot' drying front was greatest for the 200°C base temperature specimen at least for the 105°C temperature. It was also observed that for any given base temperature the hot drying front moved faster in the 10 ft. than in the 5 ft. specimen. This indicates that the magnitude of the temperatures and pore pressures, which were higher in the first 3 feet in the longer specimens influence the rate of movement of the hot drying front. Another factor that influences the rate of movement of the 'hot' drying front is the initial permeability of the concrete. The higher this initial value, the easier it is for the moisture to migrate away from the hot face when the thermal gradient is applied.

The hot drying front is preceded by one or more zones of physical saturation. This behaviour was observed by Sharp [2] in similar migration experiments using a gravel concrete. Fluctuating records of evaporable water content resulted until the drying front passed beyond the instrumentation points. However, the total water content per unit weight of mix water never fell below 0.9 in any specimen until the hot drying front had passed the instrumentation position.

Water was lost from the cold end of the specimens by evaporation drying, with an attendant weight loss. An evaporation drying front moved into the specimen, but the rate of penetration was much slower than the movement of the hot drying front. The depth of penetration did not appear to be related to the cold end temperature in the 5 ft. migration series. Figure 4 shows that the greatest depth of penetration occurred in specimen A1. This specimen had the lowest hot and cold face temperatures. This behaviour may be explained by the combination of two separate effects taking place at different rates. The evaporation drying being, at depth, a more slowly moving mass transfer process than the moisture flow caused by the higher pressures in the hotter regions; both processes operating in the same direction.

The weight loss results in Figure 5 show that the quantity of water lost from each specimen of given length increased as the hot end temperature increased. The rate of weight

loss in all the specimens was greatest at the start of the heating period. On average the specimens lost 50% of the 500 day weight loss in the first 100 days of heating, with the higher base temperature specimens losing somewhat more. The 200°C specimen lost approximately 40% of its total mix water after 500 days of heating.

Figure 6 illustrates typical spatial pore pressure distributions at various ages of heating; specimen B2. The pore pressures immediately in front of the hot drying front are above the theoretical values, which were calculated on the basis of the known temperatures and assuming no moisture migration had taken place. The higher values of pore pressure are almost certainly due to an effect caused by the accumulation of moisture. On the hot side of the drying front, the pore pressure values are spatially uniform, and lower than the theoretical estimates. This is the effect of the loss of moisture from this region. These values continue to decrease, at a steadily decreasing rate, after the hot drying front has passed.

Various values of coefficient of permeability inside the migration specimens are listed in Table 2. In specimen B2, the measured values vary from 3.39×10^{-7} cm/sec. in a sample on the hot side of the drying front to 2.44×10^{-9} cm/sec. in a sample from an area where the total water content per unit weight of mix water was greater than unity. The variation in value is of the order of 100 times, and a similar difference occurs in samples tested from specimen D4. Close examination of the results indicates that the permeability appears to be significantly affected by three factors that are interdependent. These are the elevated temperature to which the concrete is subjected; the time for which the concrete is subjected to the elevated temperature, and the evaporable water content of the concrete.

Four photographs of the concrete microstructure are presented and represent zones of different moisture contents in the migration specimens. They illustrate a number of trends. Unfortunately, there were no facilities for identifying the hydration products observed under the scanning electron microscope used, and the products have thus been identified by comparing the structures seen with those reported in previous publications.

Plate I is typical of the microstructure of the concrete on the hot side of the drying front. The hydration products appear to be affected by both the elevated temperature and loss of moisture. The "fluffy" balls, seen conglomorated together in most of the photograph, measure up to 5μm in diameter. The spaces between the balls measure between 10 μm and 25 μm.

Plate II was obtained from a sample of concrete at a point in a migration specimen where the 'hot' drying front was just passing. The 'needle' structures are similar to the material identified by Moore, Chatterji and Jeffery [15] as Calcium Silicate Hydrate. These needles join various "cores" together, giving the overall impression of a coral-like structure. The needles are about 0.2 μm thick and up to 3 μm in length. The gaps between the structures measure between 3 μm and 5 μm and appear to be continuous channels.

Plate III illustrates hydrate material from a sample of concrete where the total water content was greater than the mixing water value. The hydrate material is similar in appearance and structure to that seen in Plate II. The coral "cores" are slightly smaller in size, but the needle structures linking them are more abundant and occur in denser clusters. The gaps between the structures only measure up to 1 μm, and are less abundant than

those seen in Plate II.

Plate IV gives the microstructure in a sample of concrete cast at the same time as the migration specimens, and which remained sealed and unheated. This hydrate material represents the formation of the "coral-like" structures without the imposition of the thermal gradient and the subsequent moisture migration.

The trends indicated by these photographs are typical of all those seen in the scanning electron micrographs obtained from the migration series specimens [11]. Plate I illustrates the effect of the elevated temperature and subsequent loss of moisture, on the micro-structure of the concrete. There are no needle structures present, but the hydration products appear as small "fluffy cotton-wool" balls, scattered in a random fashion. In contrast, Plate II shows the hydration products in a sample of concrete which had experienced relatively stable 'wet' conditions and an elevated temperature for a long period of time. These conditions would explain the large hydrate growths in the photograph, that appear to be the product of enhanced concrete hydration. They also explain why the "coral-like cores" in this sample of concrete are larger in size than those seen in the concrete in Plate III, which had a total water content greater than at the time of mixing. The elevated temperature was less than the sample viewed in Plate II. Consequently, the hydration of the concrete was not enhanced to such an extent, and the size of the hydration products is smaller. However, the needle structures in Plate III occur in much denser clusters, and the gaps between the structures are smaller reflecting the influence of the higher water content. the micro-structure seen in Plate IV is a useful reference in making comparisons between the micro-structure of unheated sealed limestone concrete and that in limestone concrete that has been subjected to uniaxial moisture migration.

The variation of the linear coefficient of expansion of the limestone concrete used in the experimental programme with evaporable water content given in Figure 7 is similar in shape to a curve published by Meyers [16]. The maximum value for the coefficient obtained in the subsidiary experiment was $6.1 \times 10^{-6}/^{o}C$, and this occurred when the evaporable water content per unit weight of mix water value was 0.55 (This value is equivalent to a total water content per unit weight of mix water value of 0.895). The results for the linear coefficient of expansion compare favourably with previously reported values of $4 \times 10^{-6}/^{o}C$ by Hannant [17] and $7.5 \times 10^{-6}/^{o}C$ at 65 per cent Relative Humidity by Meyers [16] for limestone concrete. The curve shown in Figure 7 was used to adjust the shrinkage strains of the shrinkage specimen to take into account the changing moisture content. The effect of this adjustment is illustrated in Figure 8. Three transverse strains are given in this figure for disc 2, near the hot face of the shrinkage specimen. These strains are:

(1) The variation of total transverse strain with time of heating. This was deduced from the records of the total transverse movement.

(2) The variation of the shrinkage strain, calculated from the total transverse strain minus the initial thermal strain, with time of heating. In this calculation, the value of the linear coefficient of expansion was taken as $5.55 \times 10^{-6}/^{o}C$ and assumed constant throughout the heating period.

(3) The variation of shrinkage strain with time of heating calculated from the total transverse strain minus the thermal strain, adjusting the value of the linear

coefficient of expansion for the changing evaporable water content as given in Figure 7.

These curves indicate that except in the early days of heating, when the evaporable water content per unit weight of mix water was above 0.55, and moisture was migrating from the concrete, the actual shrinkage strain was less than if one assumed the linear coefficient of expansion to be of constant value. Similarly, in the parts of the specimen where moisture was accumulating, above a value of 0.55, the actual shrinkage strain was again less than if one assumed the thermal strain to be constant. This is important to design engineers of Prestressed Concrete Pressure Vessels, who must assess the effect of the moisture migration in the walls of the vessel on the properties of the concrete. An accurate knowledge of the water content and the dependence upon this parameter of the coefficient of thermal expansion is thus important if reliable predictions of shrinkage are to be made.

Figure 9 illustrates the overall behaviour of the transverse and longitudinal strains in relation to the pore pressure and total water content distributions inside the shrinkage specimen as moisture migration took place. Both the transverse and longitudinal strain distributions (adjusted to take into account the changing values of Evaporable water content) reflect the water content results. Shrinkage occurs in regions where moisture is lost, and swelling occurs in zones of water accumulation. This is similar behaviour to that observed by both England and Ross [3] and Parkinson[4] in sealed concrete specimens under a thermal gradient. In a large mass of concrete, such as a Prestressed Concrete Pressure Vessel, the concrete associated with these areas of moisture loss and accumulation will be subjected to a three dimensional system of stress; tensile in regions where moisture is lost, and compressive where there is a gain of moisture.

The shrinkage strains continued to increase on the hot side of the drying front, although the rate of increase was reduced with time. This is in agreement with the behaviour of the pore pressure and evaporable water content records for this region, and if thus clear that these parameters are interrelated. For an analysis of sealed concrete under a thermal gradient, the interrelation of these parameters must be sought if accurate prediction of the moisture migration in the concrete is to be made and its subsequent physical effects are to be understood.

5. Concluding Remarks

Moisture migration is caused by a state of non-uniform temperature, resulting in drying and attendant shrinkage in hot areas and possible physical saturation and swelling in cooler regions far removed from a free boundary. The determination of shrinkage strains is dependent upon an accurate knowledge of water content, and the influence of this parameter on the coefficient of thermal expansion of concrete. Drying and drying shrinkage at a free boundary are influenced by the magnitude of nearby temperatures and pore pressures which cause mass transfer of water towards the boundary. Only when moisture paths are long and when gradients of temperature and pressure are shallow, will evaporation drying become the influential mechanism of drying at a free face.

The photomicrographs and permeability results have provided consistent and valuable

information in relation to enhanced hydration in regions of high water content and raised temperature, and impeded hydration or degeneration coupled with higher permeability in the more severly heated zones. Permeabilities were approximately one hundred times greater in these latter regions than where an excess of water was maintained.

The combined pore pressure - shrinkage experiment has established, perhaps for the first time, that shrinkage will tend to occur whenever pore pressures are sufficient to cause significant quantities of moisture to migrate, even deep in a concrete mass. Restraint to shrinkage or swelling strains caused by moisture movement will result in a self-equilibrating state of internal stress being created, with maximum stresses occuring in the hot dry regions. In thick sections these strains will approximate to conditions of full strain restraint and could be influential in regions close to the vessel liner where pore pressures will impose an additional loading on this component.

References

[1] A.D. ROSS, J.M. ILLSTON, G.L. ENGLAND, "Short and Long-Term Deformations of Concrete as Influenced by its Physical Structure and State". Int. Conference on the Structure of Concrete, London, 1965.

[2] T.J. SHARP, "The Influence of Elevated Temperatures on the Physical Behaviour of Water in Concrete". Ph.D. Thesis, University of London, August, 1971.

[3] G.L. ENGLAND, A.D. ROSS, "Shrinkage, Moisture, and Pore Pressures in Heated Concrete". A.C.I. Conference on Concrete for Nuclear Reactors, Paper SP 34 - 42, Berlin, 1970.

[4] J.D. PARKINSON, "The Variation with Time of Water Content and Shrinkage of Concrete subjected to Thermal Gradients". Ph.D. Thesis, University of London, May, 1966.

[5] G.L. ENGLAND, T.J. SHARP, "Migration of Moisture and Pore Pressures in heated Concrete". Proc. the First International Conference on Structural Mechanics in Reactor Technology. Paper H2/4, Berlin, 1971.

[6] I.W. HORNBY, "Moisture Measurements in Mass Concrete". Conference on Prestressed Concrete Reactor Vessels, and their Thermal Insulation, Brussels, 1969.

[7] J.E. McDONALD, "An Experimental Study of Moisture Migration in Concrete", A.C.I. Conference on Concrete for Nuclear Reactors. Paper SP 34 - 45, Berlin, 1970.

[8] J. HUNDT, P. SCHIMMELWITZ, "Heat and Moisture Transfer in Concrete under the effect of a Temperature Gradient", Proc. of the Second International Conference on Structural Mechanics in Reactor Technology, Berlin, 1973.

[9] V.V. BERTERO, M. POLIVKA, "Influence of Thermal Exposures on Mechanical Characteristics of Concrete". A.C.I. Conference on Concrete for Nuclear Reactors. Paper SP 34 - 28, Berlin, 1970.

[10] D.A. CHAPMAN, G.L. ENGLAND, "Instrumentation for the Measurement of Pore Pressure and Evaporable Water Content in Concrete Specimens at Elevated Temperatures" (to be published).

[11] D.A. CHAPMAN, "A Study of the Movement of Moisture in and from Concrete at Elevated and Non-Uniform Temperatures. Ph.D. Thesis, University of London, January, 1976.

[12] D.A. CHAPMAN, G.L. ENGLAND, "The Movements of Moisture in and from Limestone Concrete at Elevated and Non-uniform temperatures; Pore Pressures and Evaporable Water". (to be published).

[13] D.A. CHAPMAN, G.L. ENGLAND, "The Movement of Moisture in and from Limestone Concrete at Elevated and Non-uniform Temperatures; Effects of Moisture Migration on the Permeability and Microstructure of Concrete". (to be published).

[14] D.A. CHAPMAN, G.L. ENGLAND, "The Movement of Moisture in and from Limestone Concrete at Elevated and Non-uniform Temperatures; Relationships between Shrinkage, Pore Pressure and Water Content", (to be published).

[15] N. MOORE, S. CHATTERJI, J.W. JEFFERY. "Morphology of Calcium Silicate Hydrate in Set Cement Paste", Journal of British Ceramics Society, Vol.5, No.1, 1968.

[16] S.L. MEYERS. "Thermal Expansion Characteristics of Hardened Cement Paste and Concrete" Proc. of the Highway Research Board, Vol. 30, No.193, 1950.

Table 1

Specimen Number	Length Ft	Age of Testing (Days)	Duration of heating (Days)	Base Temp. Deg.C.	Cold End Temp. Deg.C.	Wt. of Mix Water. lbs.	Measured Weight Loss.lbs.
A1	5'	181	582	105	41	11.31	1.390
B2	5'	182	588	125	46	11.30	2.317
C3	5'	196	573	150	50	11.44	3.129
D4	5'	195	554	175	55	11.50	3.555
E5	5'	216	531	200	76	11.40	4.366
P16	10'	239	697	150	58	20.50	7.066
Q17	10'	224	512	125	52	22.41	4.414
R18	10'	208	525	105	44	22.40	2.487
S19	10'	317	401	200	76	22.61	8.173
T20	10'	316	401	175	70	22.64	7.349

Table 2

Specimen No.	Section No.	Temperature of Section Deg. C.	$\frac{W_E}{W_T}$	$\frac{W_N}{W_T}$	Total Water	Av. D'Arcy coefficient of permeability cm/sec.
B2	3	118	0.0270	0.2850	0.3120	3.39×10^{-7}
B2	21	78	0.5450	0.3400	0.8850	8.83×10^{-9}
B2	41	52	0.6970	0.3540	1.0510	2.44×10^{-9}
D4	3	164	0.0150	0.3750	0.3900	2.23×10^{-7}
D4	17	117	0.0830	0.3600	0.4430	8.08×10^{-8}
D4	46	61.5	0.7210	0.3680	1.0890	3.92×10^{-9}

Table 3

Plate No.	Sample No.	Base Temp. Deg. C.	Temp. of Sample Deg. C.	$\frac{W_E}{W_T}$	$\frac{W_N}{W_T}$	Total Water
I	D4/13	175°C	132.5°C	0.0420	0.3620	0.4040
II	D4/26	175°C	94.0°C	0.2240	0.3660	0.5900
III	A1/30	105°C	54.0°C	0.6750	0.3550	1.0300
IV	M13/32	Room temp.	Room temp.	0.6330	0.3660	0.9990

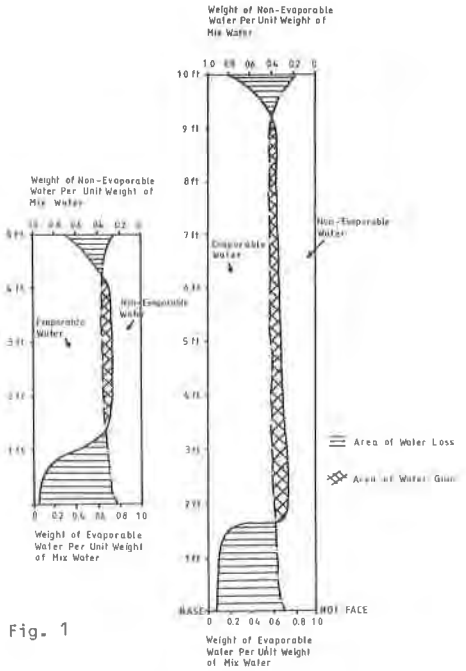

Fig. 1

PHASE DIAGRAMS FOR WATER IN CONCRETE AT 887 DAYS IN SPECIMENS OF 5ft. LENGTH AND A HOT FACE TEMPERATURE OF 125°c FROM ENGLAND AND ROSS (3)

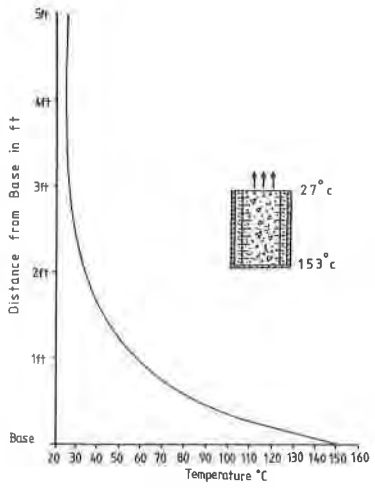

TEMPERATURE DISTRIBUTION IN SHRINKAGE SPECIMEN

Fig. 2

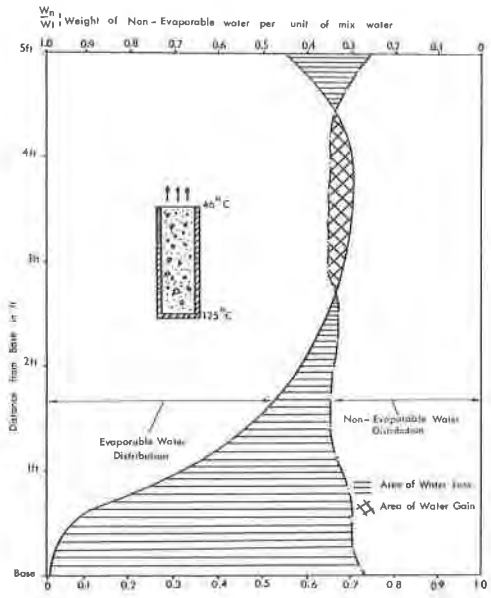

PHASE DIAGRAM FOR WATER IN SPECIMEN B2 AT THE END OF TIME OF HEATING OF 588 DAYS

Fig. 3

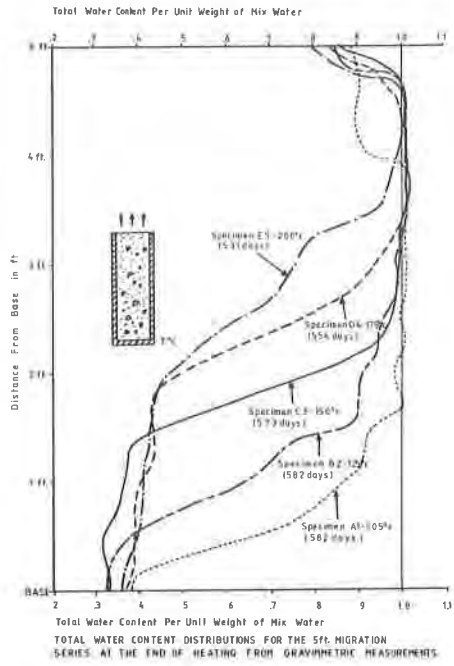

TOTAL WATER CONTENT DISTRIBUTIONS FOR THE 5ft. MIGRATION SERIES AT THE END OF HEATING FROM GRAVIMETRIC MEASUREMENTS

Fig. 4

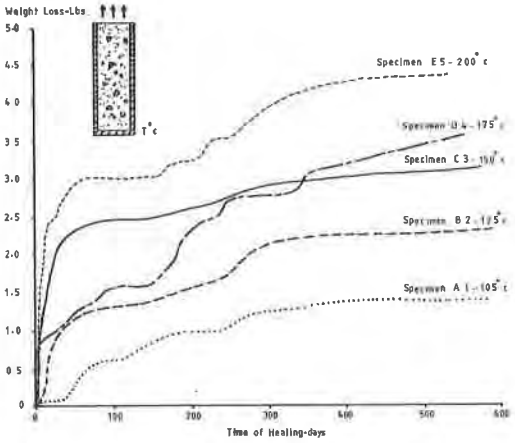

GRAPH OF WEIGHT LOSS AGAINST TIME OF HEATING FOR THE 5 FT. MIGRATION SERIES SPECIMENS

Fig. 5

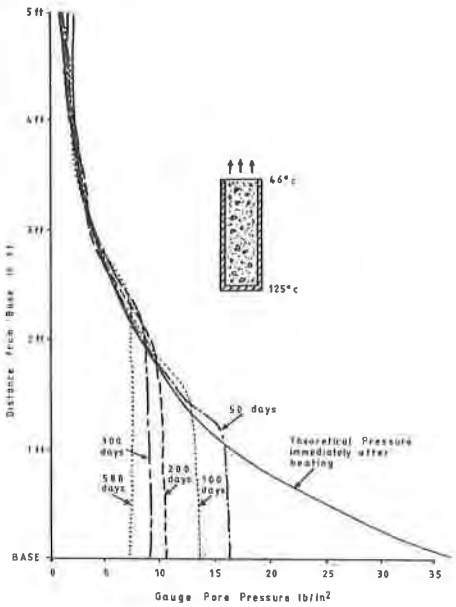

GAUGE PORE PRESSURE DISTRIBUTIONS AT VARIOUS AGES OF HEATING IN SPECIMEN B 2

Fig. 6

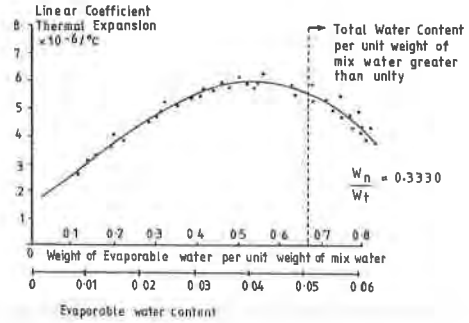

VARIATION OF LINEAR COEFFICIENT OF THERMAL EXPANSION WITH EVAPORABLE WATER CONTENT FOR THE LIMESTONE CONCRETE USED IN THE SHRINKAGE SPECIMEN

Fig. 7

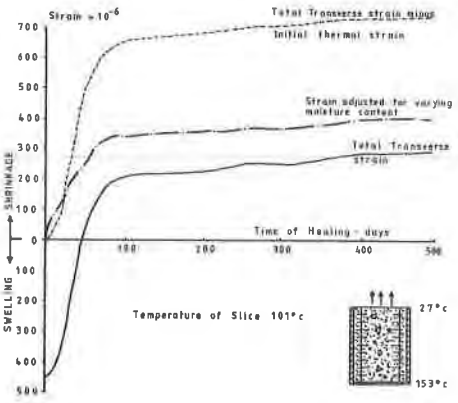

TRANSVERSE SHRINKAGE STRAINS FOR SLICE 2 IN SHRINKAGE SPECIMEN

Fig. 8

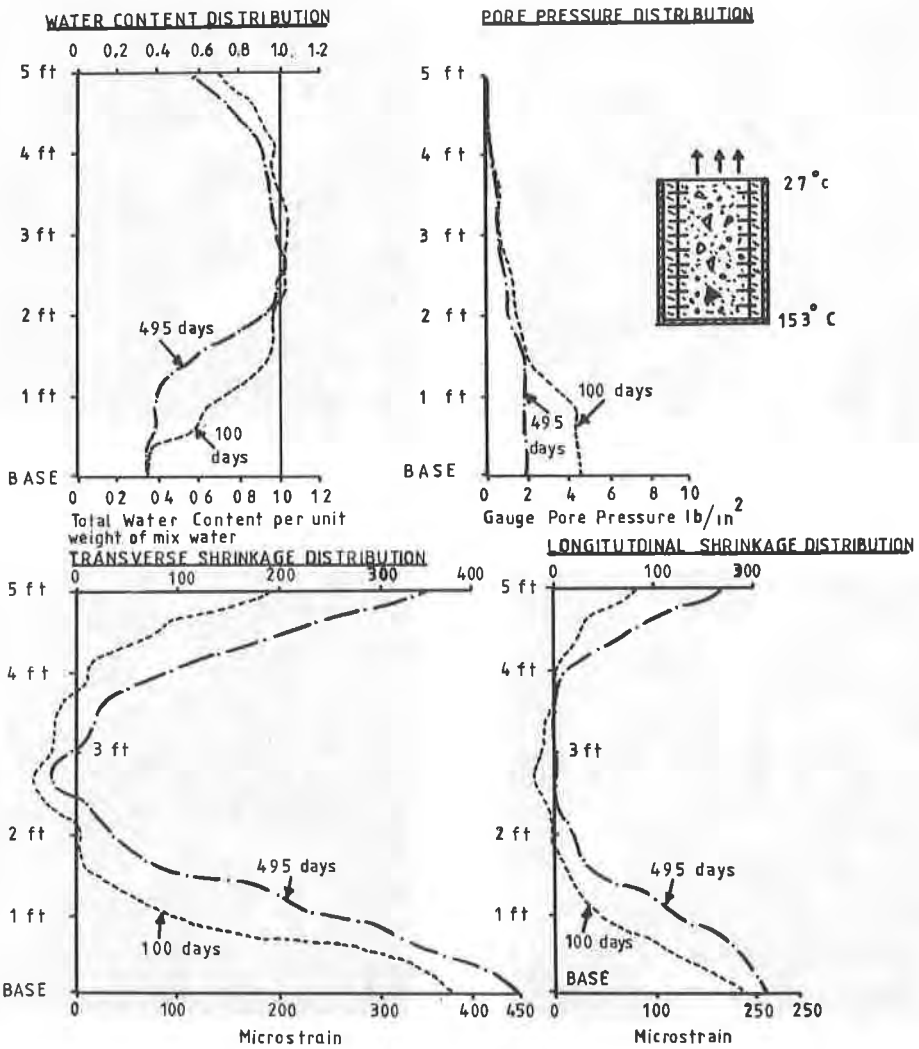

WATER CONTENT, PORE PRESSURE, TRANSVERSE AND LONGITUTDINAL SHRINKAGE DISTRIBUTIONS FOR THE SHRINKAGE SPECIMEN AFTER 100 AND 495 DAYS OF HEATING

Fig. 9

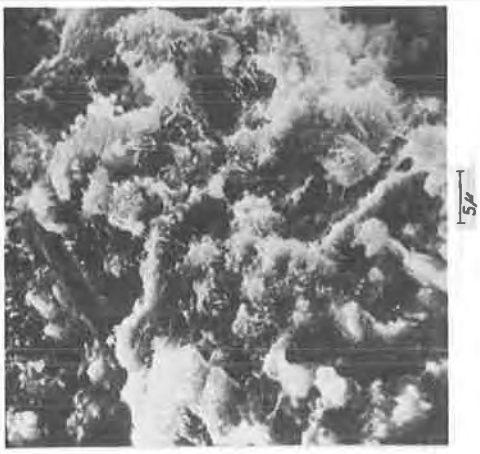

Plate I

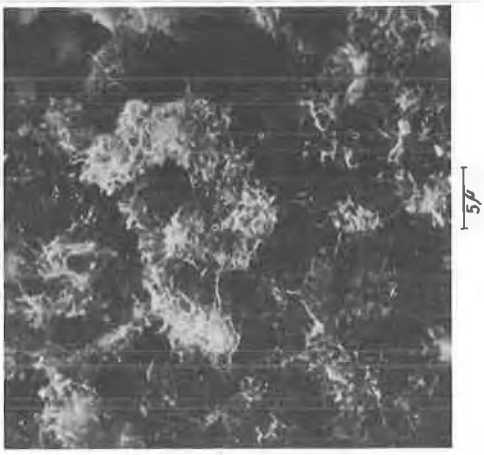

Plate II

Plate III

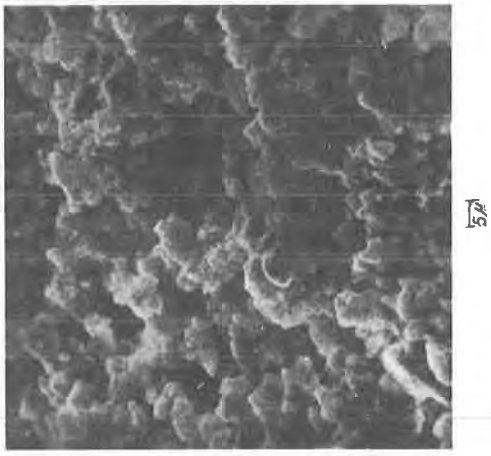

Plate IV